0026-895X/05/6805-1271–1280$20.00
MOLECULAR PHARMACOLOGY
Copyright © 2005 The American Society for Pharmacology and Experimental Therapeutics
Mol Pharmacol 68:1271–1280, 2005

Vol. 68, No. 5
15750/3059421
Printed in U.S.A.

Characterization of Determinants of Ligand Binding to the Nicotinic Acid Receptor GPR109A (HM74A/PUMA-G)

Sorin Tunaru, Jens Lättig, Jukka Kero, Gerd Krause, and Stefan Offermanns

Institute of Pharmacology, University of Heidelberg, Heidelberg, Germany (S.T., J.K., S.O.); and Forschungsinstitut für Molekulare Pharmakologie, Berlin, Germany (J.L., G.K.)

Received June 15, 2005; accepted August 10, 2005

ABSTRACT

The G-protein-coupled receptor GPR109A (HM74A/PUMA-G) has recently been shown to function as a receptor for nicotinic acid (niacin) and to mediate its antilipolytic effects. Nicotinic acid is able to strongly raise plasma levels of high-density lipoprotein cholesterol, a property that distinguishes nicotinic acid from other lipid-lowering drugs. To investigate the structural determinants of GPR109A ligand binding, we performed site-directed mutagenesis of putative ligand binding residues combined with generation of chimeric receptors consisting of GPR109A and its close relative GPR109B, which does not bind nicotinic acid. We could identify Asn86/Trp91 [transmembrane helix (TMH) 2/extracellular loop (ECL) 1], Arg111 (TMH3), Ser178 (ECL2), Phe276 (TMH7), and Tyr284 (TMH7) as amino acid residues critical for binding of nicotinic acid. Together with data from molecular modeling studies, our data suggest that the ligand binding pocket for nicotinic acid of GPR109A is distinct from that of most other group A receptors. Although Arg111 at TMH3 serves as the basic anchor point for the carboxylate ligands, the ring system of nicotinic acid is embedded between Trp91 at the junction TMH2/ECL1 and Phe276/Tyr284 at TMH7. The heterocyclic ring is also bound to Ser178 at ECL2 via an H-bond. These data will facilitate the design of new antidyslipidemic drugs acting via GPR109A.

The water soluble B-complex vitamin nicotinic acid (niacin) has been shown to decrease plasma concentrations of total cholesterol, free fatty acids, and triglycerides when given at pharmacological doses to humans (Altschul et al., 1955; Carlson and Oro, 1962). For decades, these effects have been used to treat different dyslipidemic disorders (Olsson, 1994; Knopp, 1999). In contrast to other lipid-lowering drugs, nicotinic acid strongly raises high-density lipoprotein cholesterol levels (Blum et al., 1977; Shepherd et al., 1979). However, relatively high doses of nicotinic acid have to be administered, and the beneficial effects on lipid metabolism are accompanied by mostly harmless but disturbing side effects such as flushing, decreased glucose tolerance, or gastrointestinal effects (Olsson, 1994). Despite its long use in clinical practice, the exact mechanism of nicotinic acid-induced effects on lipid metabolism is still not completely understood. However, the inhibition of fat cell lipolysis via the activation of a G_i-coupled receptor and subsequent inhibition of cAMP formation (Aktories et al., 1980, 1982) has been postulated to play an important role (Tornvall et al., 1990).

A G-protein-coupled receptor that binds nicotinic acid with the expected affinity has been identified (Soga et al., 2003; Tunaru et al., 2003; Wise et al., 2003). The receptor termed GPR109A (HM74A in human and PUMA-G in mice) is expressed in adipocytes and immune cells and couples to G-proteins of the G_i family. Activation of the receptor by nicotinic acid decreases the activity of hormone-sensitive lipase via lowering of cAMP levels, which results in a reduced hydrolysis of triglycerides to free fatty acids. In mice lacking the murine form of the nicotinic acid receptor, the antilipolytic effects of nicotinic acid, which result in a decrease in free fatty acid and triglyceride plasma levels, are abrogated (Tunaru et al., 2003). Thus, GPR109A (HM74A/PUMA-G) is the receptor mediating the antilipolytic effects of nicotinic acid. Bioinformatic data indicate that GPR109A is a member of a subfamily of G-protein-coupled receptors that comprises GPR109A (HM74A/PUMA-G) and GPR81, both of which exist in humans and in rodent species. In addition, a third member of this receptor family, GPR109B (HM74), has been found in humans, but not in mice and rats (Soga et al., 2003; Wise et al., 2003). GPR109A, GPR81, and GPR109B are

This work was supported by the Deutsche Forschungsgemeinschaft (S.O.).
Article, publication date, and citation information can be found at http://molpharm.aspetjournals.org.
doi:10.1124/mol.105.015750.

ABBREVIATIONS: acifran, 4,5-dihydro-5-methyl-4-oxo-5-phenyl-2-furancarboxylic acid; CHO, Chinese hamster ovary; CHAPS, 3-[(3-cholamidopropyl)dimethylammonio]propanesulfonate; PBS, phosphate-buffered saline; ELISA, enzyme-linked immunosorbent assay; TMH, transmembrane helix; TM, transmembrane; ECL, extracellular loop; ELISA, enzyme-linked immunosorbent assay.

colocalized on human chromosome 12q24.31 and are most likely to be the result of gene duplications (Zellner et al., 2005). It is interesting that nicotinic acid and related compounds such as acipimox (5-methylpyrazine carboxylic acid 4-oxide) are only able to bind to GPR109A (Soga et al., 2003; Wise et al., 2003). In contrast, acifran (4,5-dihydro-5-methyl-4-oxo-5-phenyl-2-furancarboxylic acid), which also induces changes in lipoprotein profile similar to those induced by nicotinic acid (Cayen et al., 1982; LaRosa et al., 1987) is an agonist on both GPR109A and GPR109B, indicating that GPR109B is a functional G-protein-coupled receptor (Wise et al., 2003). No ligand has been described for GPR81 so far.

Because the nicotinic acid receptor is of great interest as a target for new antidyslipidemic drugs, we have aimed in the present study to characterize the structural requirements of GPR109A for binding of nicotinic acid. Based on the high degree of homology between the human high-affinity nicotinic acid receptor GPR109A and the receptor GPR109B, which has only very low affinity for nicotinic acid, we used an iterative approach combining site-directed mutagenesis, analysis of GPR109A/GPR109B chimeras, and structural modeling to characterize the nicotinic acid-binding pocket on GPR109A.

Materials and Methods

Materials. Nicotinic acid (pyridine-3-carboxylic acid) was from Sigma (St. Louis, MO), and acifran was from Tocris Cookson Inc. (Bristol, UK).

Calcium Mobilization. CHO-K1 cells stably transfected with a calcium-sensitive bioluminescent fusion protein consisting of aequorin and green fluorescent protein (Baubet et al., 2000) were seeded in 96-well plates and were transfected with indicated cDNAs or control DNA (50 ng/well) using FuGENE6 reagent (Roche Diagnostics, Mannheim, Germany). Two days after transfection, cells were loaded with 5 μM coelenterazine *h* (Biotium, Hayward, CA) in calcium-free Hanks' balanced salt solution containing 10 mM HEPES, pH 7.4, for 3.5 h at 37°C. Forty-five minutes before experiments, the buffer was replaced with Hanks' balanced salt solution containing 1.8 mM $CaCl_2$. Measurements were performed by using a luminometer plate reader (Luminoskan Ascent; Thermo Electron Corporation, Waltham, MA).

Radioligand Binding. Equilibrium binding of ^{3}H-labeled nicotinic acid (50 Ci/mmol; American Radiolabeled Chemicals, St. Louis, MO) was performed on 30 μg of membranes from human embryonic kidney 293T cells expressing wild-type or mutant receptors in a total volume of 250 μl of binding buffer [50 mM Tris-HCl, pH 7.4, 2 mM $MgCl_2$, and 0.02% (v/v) CHAPS] as described previously (Tunaru et al., 2003). After 4 h of incubation at 25°C, unbound and membrane-bound radioactivity were separated by filtration of the samples through nitrocellulose filters, followed by two washing steps with 4 ml of ice-cold binding buffer. Nonspecific binding was determined in the presence of 200 μM unlabeled nicotinic acid.

Site-Directed Mutagenesis, Generation of Receptor Chimeras. Specific mutations introduced in GPR109A receptors were carried out based on QuikChange site-directed mutagenesis procedure (Stratagene, La Jolla, CA) using *Pfu Turbo* as a proofreading DNA polymerase. A receptor version carrying a FLAG-tag at the N terminus was used as a template for mutagenesis. Correct mutagenesis was confirmed by DNA sequencing. For generation of receptor chimeras, GPR109A and GPR109B receptor cDNAs were cut with BglII endonuclease. BglII has recognition sites within both receptor cDNAs that corresponds to a location between amino acids Ile139 and Ser140 of GPR109A. Additional point mutations were introduced in chimeras by site-directed mutagenesis as described above.

Determination of Receptor Expression and Localization. CHO/G5A cells grown on glass coverslides in six-well plates were transfected with the indicated N-terminally FLAG-tagged receptors using FuGENE (Roche Diagnostics). Twenty-four hours later, cells were transferred onto ice, and the medium was removed. Cells were washed two times with ice-cold PBS and were then fixed for 30 min in 4% PFA in PBS at room temperature. To reduce the nonspecific binding of the antibody, cells were blocked for 30 min in 4% fetal bovine serum in PBS at room temperature, followed by incubation for 2 h at room temperature with anti-Flag antibody (Sigma). After three washing steps with 2% BSA in PBS, cells were labeled with anti-mouse tetramethylrhodamine B isothiocyanate-conjugated secondary antibody (Jackson ImmunoResearch Laboratories Inc., West Grove, PA) for 30 min at room temperature. Cells were washed six times with Tris buffer (50 mM Tris and 150 mM NaCl, pH 7.5) and stained cells were visualized using a confocal imaging system (DM IRE2; Leica, Wetzlar, Germany).

Cell surface expression of wild-type and mutant FLAG-tagged receptors was assessed by enzyme-linked immunosorbent assay (ELISA) using Anti-FLAG antibody and horseradish peroxidase-conjugated secondary antibody (GE Healthcare, Little Chalfont, Buckinghamshire, UK). Light generated by incubation with horseradish peroxidase substrate (Roche Diagnostics) was measured by using an Ascent Luminometer (Thermo Electron).

Homology Modeling and Ligand Docking. To generate a structural model for GPR109A/B, we adopted the X-ray structure of rhodopsin (Teller et al., 2001) from entry 1HZX of the Protein Data Base (PDB) (Berman et al., 2000) as a template. Several receptor-specific corrections were made based on sequence alignment investigations (SeqLab, Wisconsin Package Version 10.2; Accelrys Inc. San Diego, CA). At the N-terminal tail, the two consecutive cysteines Cys18 and Cys19 are forming two additional disulfide bridges toward extracellular loop (ECL) 2 (C18-ECL2:C183) and ECL3 (C19-ECL3:C266), respectively. For transmembrane helices (TMH) 2, a structural "bulge" of Rhodopsin caused by side chain/backbone interaction of three consecutive threonines in the rhodopsin structure would localize Asp85/Asn86 at the membrane-oriented phase of the helix. New construction of the TMH2/ECL1 junction avoids the bulge structure of rhodopsin and considers a proline kink from other TM structures (Sansom and Weinstein, 2000). The new conformation is similar to that in chemokine receptor models (proline is located on the same sequence position as in GPR109A/B). In addition, at TMH5, a minor change of orientation (10- to 15-degree twist) of the N-terminal half of TMH5 was generated as a result of different residues compared with rhodopsin before the proline kink at Pro200. The length of ECL3 was extended by an additional helix turn at TMH6 because of more residues in GPR109A/B than in the rhodopsin template. Gaps of missing residues in the intracellular loops of the template structure were closed by the "Loop Search" tool implemented in Sybyl 6.8 (Tripos Inc., St. Louis, MO) using GPR109A/B sequence. Concerning the orientation of ECL2, we started with two different models: one with the original rhodopsin fold in counterclockwise order of residues around Cys177 and a second model with reversed, clockwise order of ECL2 residues around Cys177 by preserving the β-strand motifs. This results in a suitable geometry for pairing the additional disulfide bridges. After model generation, the structures were minimized using Amber4.1 force field and Amber95_Protein_ALL charges. In a first step, the ligands are manually docked according to the potential interaction points suggested by the results obtained with the receptor mutants. In a second step, the stability of the ligand in the binding site was studied by molecular dynamics runs in a water-vacuum-water box system (ter Laak and Kuhne, 1999) without any restrains (1.0 ns, periodic boundary box, charges neutralized by adding chlorine ions) using AMBER 7.0 (Case et al., 2002). The quality of the model and stability is validated by checking the geometry by PROCHECK (Laskowski et al., 1996) and the stability during the molecular dynamics run (overall backbone root mean square deviation, 1.7 Å).

Results

Both the human nicotinic acid receptor GPR109A and the paralogous receptor GPR109B are functional G-protein-coupled receptors that can be activated by the furan-carboxylic acid derivate acifran (Wise et al., 2003). In contrast, pyridine-3-carboxylic acid (nicotinic acid), as well as pyrazine-carboxylic acid derivatives such as acipimox, function as high-affinity agonists only on GPR109A but not on GPR109B (Soga et al., 2003; Wise et al., 2003). In addition to a shorter C terminus, GPR109A differs from GPR109B in only 17 amino acid residues that cluster around ECL1 and -2 (Fig. 1). It is likely that these amino acid residues, 14 of which are conserved in human, mouse, and rat versions of the receptor, are critically involved in ligand binding. We have therefore systematically mutated each of these amino acid residues in GPR109A into the corresponding residue of GPR109B. Nicotinic acid-induced activation of mutant receptors was tested in cells co-expressing receptor mutants and the promiscuous G-protein α-subunit $G\alpha_{15}$ in a Ca^{2+} reporter assay as described previously (Tunaru et al., 2003). All receptor mutants were N-terminally tagged with the FLAG epitope, and expression as well as membrane localization was verified by confocal microscopy and ELISA (see *Materials and Methods*). Of the 14 mutants tested, only Asn86Y, Trp91S, and Ser178I showed a severely reduced ability to respond to nicotinic acid (Fig. 2A; Table 1). All other single amino acid mutants showed unaltered or only very slightly reduced EC_{50} values for nicotinic acid-induced Ca^{2+}-mobilization. The three mutants, which only weakly responded to nicotinic acid, were well expressed and showed membranous localization (Fig. 2G; Table 1). In addition, they still responded to acifran. It is noteworthy that the potency of acifran to act via these three mutants was reduced to the level observed for GPR109B (Fig. 2B; Table 1). Together, these data indicate that the mutants were functionally active. We then performed radioligand binding assays using ^{3}H-labeled nicotinic acid (Table 1). All mutants (N86Y, W91S, and S178I) showed severely reduced binding affinities for nicotinic acid. Thus, asparagine 86, tryptophan 91, and serine 178 of GPR109A are required for high-affinity binding of nicotinic acid but are not necessary for acifran-induced receptor activation.

Because all known ligands for GPR109A carry a carboxylate group, it seemed likely that a basic residue in GPR109A is important for binding of carboxylic acid ligands. This is

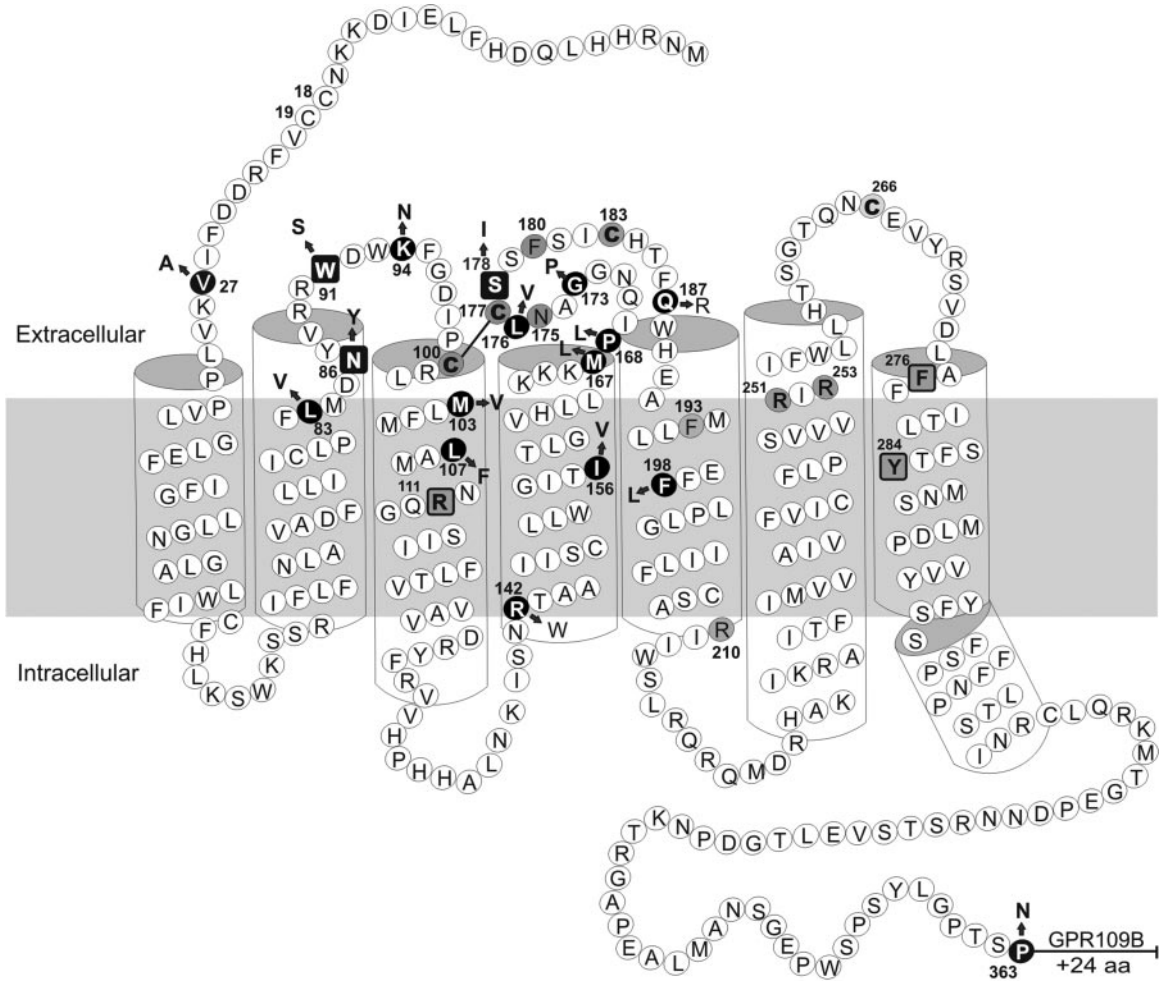

Fig. 1. Secondary structure of the human nicotinic acid receptor GPR109A. White amino acid symbols on black circles and squares indicate residues in GPR109A that differ from GPR109B. The arrows point to the corresponding amino acid in GPR109B. Gray circles and squares indicate amino acid residues of GPR109A that, in addition, have been mutated in this study. Shown in squares are those residues that showed a significant difference in nicotinic acid binding when mutated in GPR109A. Extracellular, transmembrane, and cytoplasmic regions are based on the structure of rhodopsin. A straight line indicates the disulfide bond found in the extracellular part of the receptor. GPR109B has a C terminus that is extended by 24 amino acids.

supported by the fact that any change or substitution at the carboxylic acid moiety of nicotinic acid, such as in nicotinamide, completely abrogates its pharmacological activity (Soga et al., 2003; Tunaru et al., 2003; Wise et al., 2003). We identified four arginine residues in TMH as candidates that may provide a binding environment for the carboxylate groups of GPR109A receptor ligands (Fig. 1). To test their potential involvement in nicotinic acid binding, we mutated arginine residues 111, 210, 251, and 253 into alanine. Although the effects of nicotinic acid and acifran on the R253A and R210A mutants were indistinguishable from those on wild-type receptor, the potencies of both agonists were re-

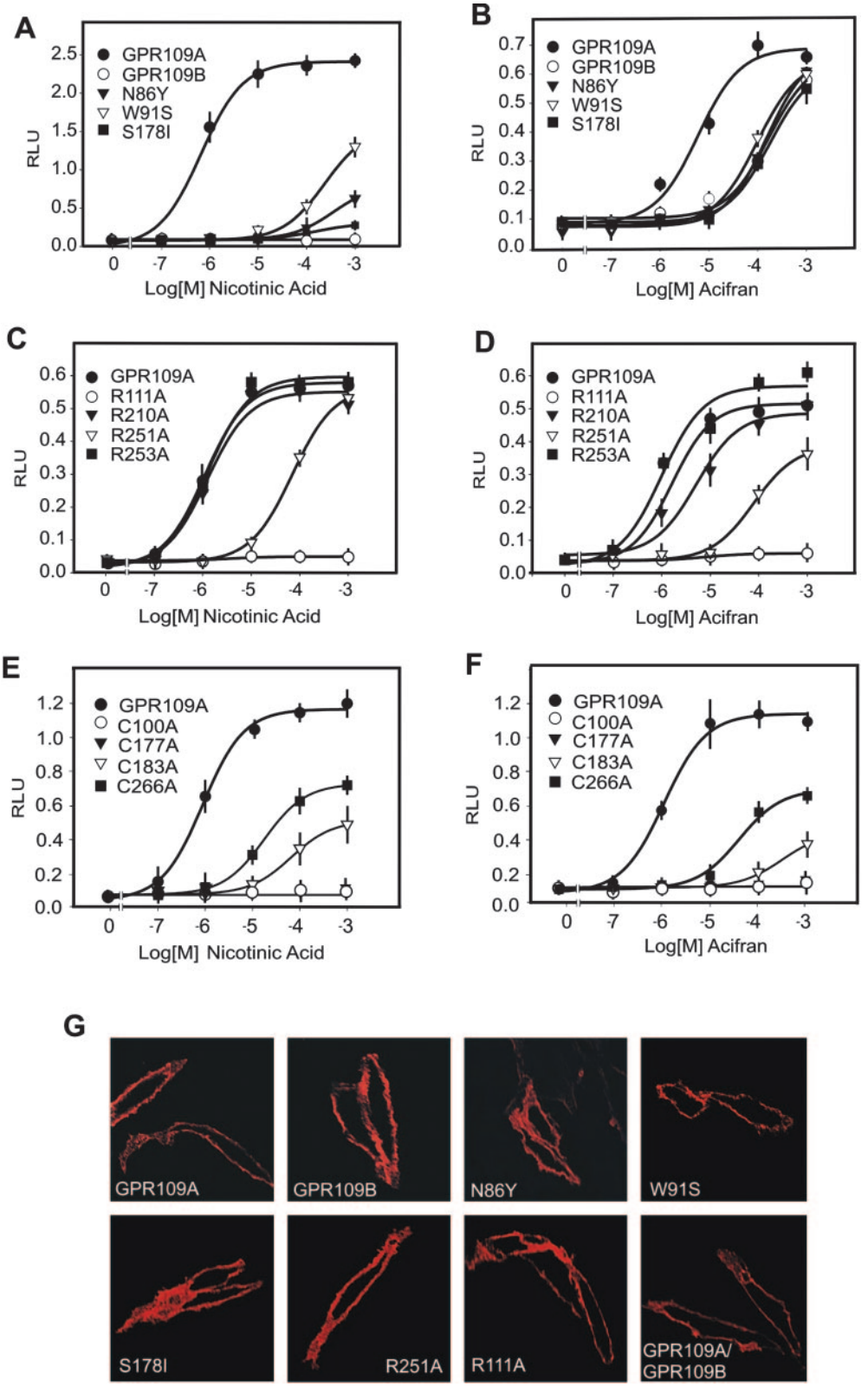

Fig. 2. Concentration-dependent changes in $[Ca^{2+}]_i$ evoked in CHO-K1 cells expressing GPR109B, GPR109A, or the indicated mutants of GPR109A by nicotinic acid (A, C, and E) or acifran (B, D, and F). RLU, relative light units. Shown are mean values ± S.D. of at least three independently performed experiments. G, confocal images of CHO-K1 cells transfected with the indicated wild-type and mutant receptors. Staining was performed using an anti-FLAG antibody recognizing the N-terminal FLAG tag of the receptors.

duced when tested on the GPR109A mutant R251A. However, no receptor activation at all could be observed when nicotinic acid and acifran were tested on the GPR109A mutant R111A (Fig. 2, C and D; Table 1). Subsequent radioligand binding studies showed that the R251A mutant had a somewhat reduced affinity for nicotinic acid, whereas R111A lost its ability to bind nicotinic acid (Table 1). The R111A mutant was normally expressed and localized to the plasma membrane as shown by confocal microscopy and ELISA (Table 1, Fig. 2G). This suggests that arginine 111, which is localized in TMH3 of GPR109A and GPR109B, is crucial for ligand-dependent receptor activation by contributing to the binding pocket of the receptor. The corresponding position 3.33 (Ballesteros and Weinstein, 1992) in many GPCRs has been shown to be involved in ligand binding (Gether, 2000).

As is typical for class A G-protein-coupled receptors, GPR109A has a cysteine residue at the extracellular end of TMH3 (C3.25) that forms a disulfide bond with a cysteine residue in the ECL2. Removal of the disulfide bond by mutagenesis has been shown to severely interfere with the function of GPCRs (Savarese et al., 1992; Noda et al., 1994). GPR109A has two cysteine residues, Cys177 and Cys183, in the second extracellular loop (Fig. 1). A C183A mutation in GPR109A rendered the receptor still responsive to nicotinic acid, although the potency was severely reduced, whereas C100A and C177A mutations resulted in a receptor that was completely unable to respond to nicotinic acid or acifran (Table 1; Fig. 2, E and F). Analysis of receptor expression revealed that both the C100A and the C177A mutants of GPR109A were only poorly expressed. This indicates that the disulfide bond conserved in class A GPCRs (Gether, 2000) is formed between cysteine residues 100 and 177 of GPR109A. The reduced potency of nicotinic acid at the C183A mutant of GPR109A can be explained by an additional disulfide bond established between ECL2 and one of the cysteines at the N-terminal tail, which may stabilize the conformation of ECL2.

The three residues that are different in GPR109A and GPR109B that were found to be essential for binding of nicotinic acid to GPR109A are either at the junction of TMH2 and the first ECL (Asn86 and Trp91) or in the second ECL (Ser178). This suggests that both junction TMH2/ECL1 and ECL2 are part of the binding site for nicotinic acid in GPR109A. To gain further insight into the structural requirements of GPR109A for binding of nicotinic acid, we generated chimeras of GPR109A and GPR109B. The chimeras were constructed such that the first three TM regions, including the junction TMH2/ECL1, were from one receptor, whereas the C-terminal four TM regions, including the second ECL, were from the corresponding homologous receptor (see *Materials and Methods*; Fig. 3A). The unselective agonist acifran was still able to activate both chimeras, although the potency of acifran toward the GPR109B/GPR109A chimera was somewhat reduced (Fig. 3, B and D). In contrast, both receptor chimeras were completely unresponsive to nicotinic acid (Fig. 3, B and C). Radioligand binding assays showed that none of the chimeras bound nicotinic acid (Fig. 3B). To further characterize the involvement of the junction TMH2/ECL1 and of ECL2 in binding of the receptor to nicotinic acid, we mutationally reintroduced the GPR109A-specific extracellular residues required for nicotinic acid binding (Asn86, Trp91, and Ser178) into the GPR109B portion

TABLE 1

Nicotinic acid and acifran evoked Ca^{2+} responses (EC_{50}) and nicotinic acid binding affinity (K_d) for GPR109A mutants

Shown are data for GPR109A and GPR109B wild-type receptors as well as for the indicated GPR109A mutants. The EC_{50} values of nicotinic acid-induced increases in $[Ca^{2+}]_i$ were determined in CHO-K1 cells expressing $G\alpha_{15}$ and the indicated wild-type or mutant receptors. Saturation binding results are the mean ± S.D. of at least three experiments; shown are the K_D and B_{max} values determined by Scatchard analysis of [^{3}H]nicotinic acid binding saturation isotherms. Relative cell surface expression levels of wild-type and GPR109A receptor mutants were determined by ELISA assay in nonpermeabilized CHO-K1 cells (see *Materials and Methods*).

	EC_{50}		[^{3}H]Nicotinic Acid Binding		Surface Expression
	Nicotinic Acid	Acifran	K_d	B_{max}	
	μM		*nM*	*pmol/mg*	*RLU*
WT receptors					
GPR109A	0.7 ± 0.2	1.9 ± 0.4	60 ± 8	3.36 ± 0.45	39 ± 2.21
GPR109B	Inactive	90 ± 12	>500		42.4 ± 5.09
GPR109A mutants					
L83V	3 ± 0.5	2 ± 0.3			
N86Y	>100	88 ± 20	>500		45.27 ± 1.91
W91S	>100	96.8 ± 10	>500		51.24 ± 4.9
K94N	1.4 ± 0.8	4 ± 0.7			
M103V	5.3 ± 1.1	2.2 ± 0.5			
L107F	3.1 ± 0.5	2.9 ± 0.3			
R142W	1 ± 0.3	4.3 ± 0.5			
I156V	0.5 ± 0.1	2.8 ± 0.4			
M167L	2.3 ± 0.3	5.6 ± 0.2			
P168L	2.3 ± 0.4	4.7 ± 0.6			
G173P	1.1 ± 0.2	2.4 ± 0.3			
L176V	3 ± 0.4	18.7 ± 2			
S178I	>100	93.1 ± 15	>500		49 ± 2.8
F198L	0.7 ± 0.1	2 ± 0.1			
R111A	Inactive	Inactive	>500		39.27 ± 3.01
R210A	0.8 ± 0.2	6 ± 1.5			
R251A	70 ± 12	80 ± 14	351 ± 22	4.1 ± 0.21	40.2 ± 3.4
R253A	0.9 ± 0.1	1.9 ± 0.4			
C100A	Low expression	Low expression	Low expression		3.5 ± 0.27
C177A	Low expression	Low expression	Low expression		0.51 ± 0.02
C183A	>100	>100	>500		20.37 ± 1.7
C266A	20 ± 3	40 ± 9	160 ± 13	3.03 ± 0.25	39.87 ± 3.1

of the GPR109A/GPR109B chimeras (see Fig. 3A). The GPR109B(Y86N,S91W)/GPR109A chimera was then again able to bind and respond to nicotinic acid. Likewise, the GPR109A/GPR109B(I178S) chimera gained responsiveness and binding toward nicotinic acid (Fig. 3, B and C). B_{max} values were 3.98 ± 0.34 pmol/mg for GPR109B(Y86N,S91W)/GPR109A and 4.01 ± 0.23 pmol/mg for GPR109A/GPR109B(I178S). All mutants were normally expressed (Fig. 2G; data not shown). These data clearly support the notion that Asn86, Trp91, and Ser178 in the junction of TMH2/ECL1 and in ECL2 of GPR109A are critically involved in nicotinic acid binding.

Our modified homology model of GPR109A, including the reversed order of ECL2, was most consistent with the experimental data, where the residues Asn86, Trp91, and Ser178 are located in close spatial proximity between the junction TMH2/ECL1 and ECL2. The mutation-sensitive basic side chain Arg111 (TMH3) is located in the interior center of the traditional binding area for the majority of G-protein-coupled receptor ligands. Docking studies, by anchoring the acidic group of nicotinic acid toward the most sensitive basic residue (Arg111 at TMH3 in the center of the receptor), allows us to define two potential binding areas for the very small ligand. In binding site I, the pyridine ring of nicotinic acid is embedded between the aromatic rings of Trp91 (junction TMH2/ECL1), Phe276 (TMH7), and Tyr284 (TMH7), whereas the ring nitrogen is simultaneously bound to Ser178 at ECL2 via an H-bond. The suitable side chain orientation of the two aromatic side chains Trp91 and Phe276 are, in the case of Trp91 (TMH2/ECL1), restrained by Asn86 (TMH2) via H-bond and, in the case of Phe276 (TMH7), restrained by Phe180 (ECL2) via aromatic interactions (Fig. 4, A and B). Binding site II would be localized at the interior receptor cleft between TMH3, TMH6, and TMH5 at the extracellular half of the transmembrane region, a common ligand binding region for the majority of small ligands such as the biogenic amine receptors of class A GPCRs. The locations of nearly all sensitive mutants for binding nicotinic acid (Table 1) are spatially distributed at site I (Arg111, Asn86, Trp91, Ser178) of the GPR109A model. The mutation of Arg251 that is localized at site II had only a weak effect on ligand binding, and ligand-induced signaling might be based on an indirect effect. (Table 1; Fig. 2).

From analyses of crystal structures of nicotinic acid bound at diverse prokaryotic proteins [such as nicotinate mononucleotide dimethylbenzimidazole phosphoribosyltransferase (PDB code 1D0V) (Cheong et al., 1999), dihydropteridine reductase (PDB code 1ICR) (Lovering et al., 2001), nicotinate nucleotide dimethylbenzimidazole phosphoribosyltransferase (PDB code 1JHA) (Cheong et al., 2001), dihydrodipicolinate reductase (PDB code 1DRV) (Reddy et al., 1996), and the plant protein ferric soybean leghemoglobin (PDB code 1FSL) (Ellis et al., 1997)], it is evident that the pyridine ring system of the ligand is always bound near aromatic side chains of the protein. Following the structural homology paradigm, we assumed that the binding pocket of GPR109A is also coated by aromatic side chain(s) as an additional binding partner for nicotinic acid. According to our ligand/receptor interaction

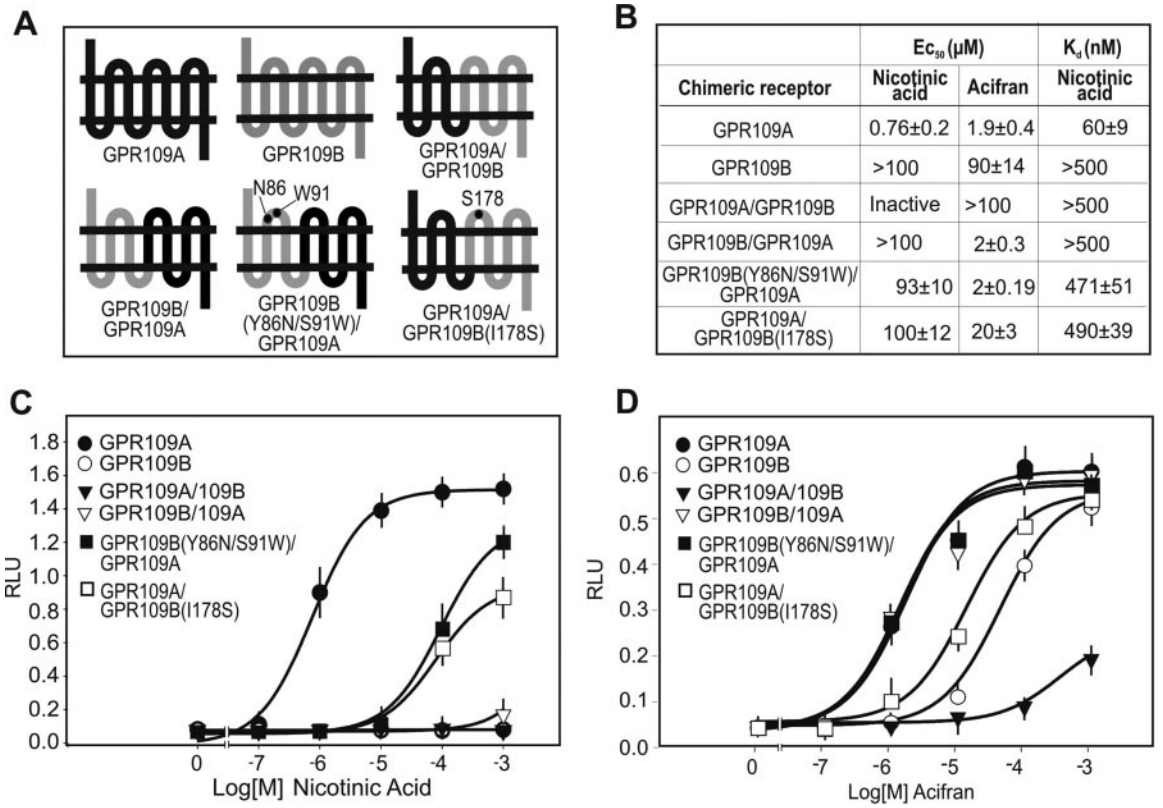

Chimeric receptor	Ec_{50} (μM) Nicotinic acid	Ec_{50} (μM) Acifran	K_d (nM) Nicotinic acid
GPR109A	0.76±0.2	1.9±0.4	60±9
GPR109B	>100	90±14	>500
GPR109A/GPR109B	Inactive	>100	>500
GPR109B/GPR109A	>100	2±0.3	>500
GPR109B(Y86N/S91W)/GPR109A	93±10	2±0.19	471±51
GPR109A/GPR109B(I178S)	100±12	20±3	490±39

Fig. 3. A, structure of the chimeric GPR109B/GPR109A receptors. Black indicates sequences and residues from GPR109A; gray indicates sequences from GPR109B. B, nicotinic acid- and acifran-evoked Ca^{2+} responses (EC_{50}) and nicotinic acid binding K_d) for chimeric GPR109A and GPR109B receptors. Effect of increasing concentrations of nicotinic acid (C) or acifran (D) on the free intracellular Ca^{2+}-concentration in CHO-K1 cells expressing the promiscuous G-protein $G\alpha_{15}$ together with GPR109B, GPR109A, or the indicated chimeric receptors. Shown are mean values ± S.D. of at least three independently performed experiments.

model, in addition to Trp91, Phe276 (TMH7) and Tyr284 (TMH7) were also predicted to be direct interaction partners. Residue Phe180 (ECL2) was predicted to be an indirect aromatic interaction partner at binding site I (Fig. 4B), whereas residue Phe193 (TMH5) would be a possible partner at a potential binding site II. To study whether the aromatic residues are required for ligand induced signaling and to distinguish between binding sites I and II, leucine and alanine mutants of these aromatic residues were generated. Indeed, mutation of the aromatic residues Phe276 (TMH7) and Tyr284 (TMH7) at binding site I to alanine or leucine had the strongest effects on binding of nicotinic acid and

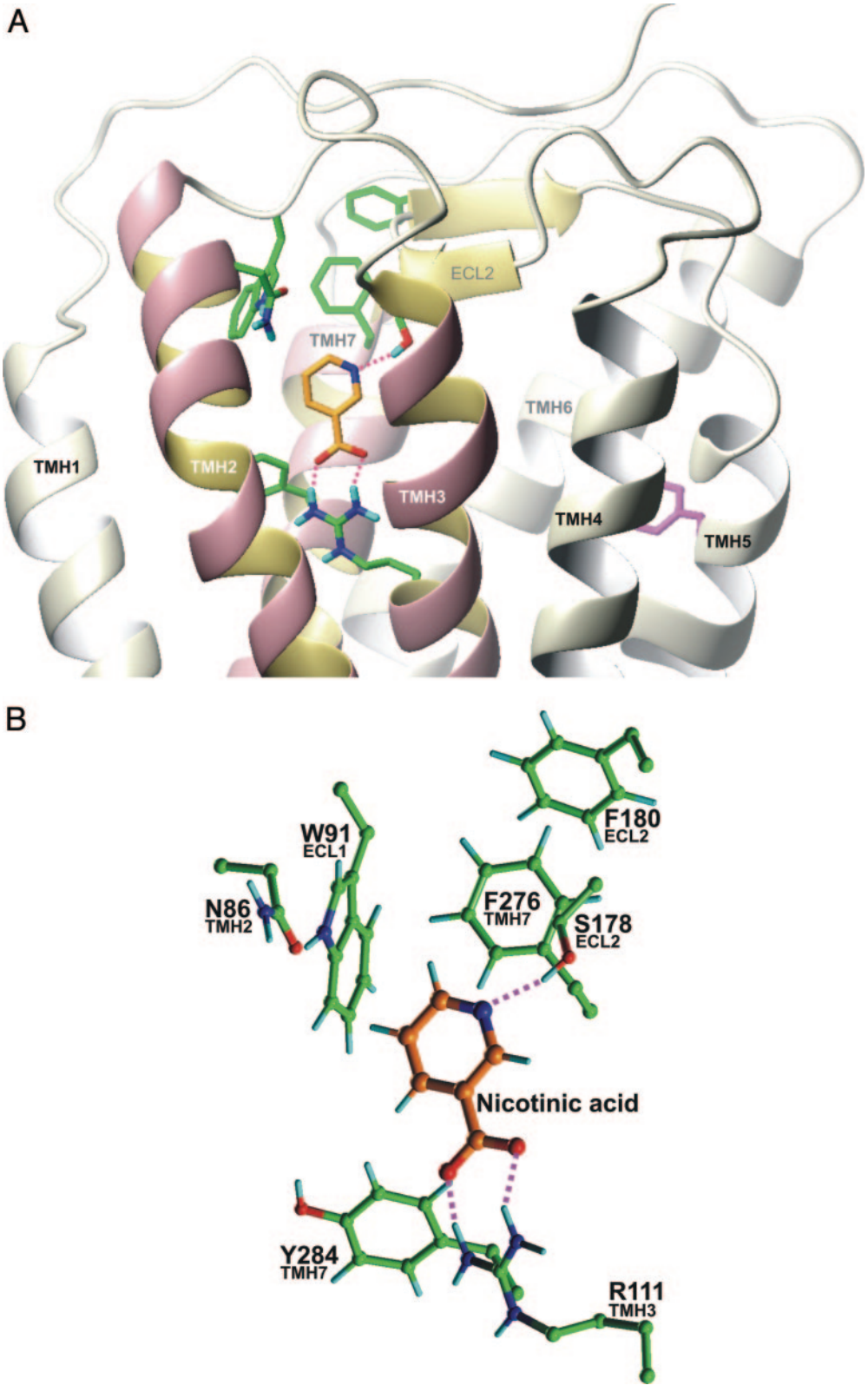

Fig. 4. Interaction model of nicotinic acid (orange) at the binding site (green residues) of GPR109A receptor. Stable conformation after a 1.0-ns molecular dynamics run. A, the binding site of nicotinic acid is located between TMH2, -3, and -7 (pink/yellow ribbon). Our data do not support an alternative binding site between TMH3, -4, -5, and -6 (e.g., magenta residue F193). B, close-up view of the binding site. Acidic group of nicotinic acid (orange) interacts with the basic anchor point Arg111 at TMH3, whereas the pyridine ring is embedded between Trp91 at the junction TMH2/ECL1, Phe276, and Tyr284 at TMH7. The pyridine nitrogen is also bound to Ser178 at ECL2 via an H-bond. Asn86 (TMH2) restrains the orientation of Trp91 by hydrogen bond, and Phe180 (ECL2) restrains the orientation ofPhe276 by aromatic interactions leading to a suitable and rigid binding cleft.

acifran, indicating a direct effect on the ligand binding site (Table 2) via aromatic interactions. The alanine mutants of Phe180 and Phe193 had the same phenotypes, whereas F180L and F193L mutants were only slightly affected in their ability to bind ligand. This indicates indirect effects of alanine mutants on the ligand binding site and provides additional support for binding site I, because F193, at TMH5, is far from binding site I and would be the only residue located at a hypothetical binding site II (Fig. 4A). All mutants have expression levels similar to wild type (data not shown). The suggested additional mutations of aromatic residues further support the binding site I and confirmed the direct and indirect effects of aromatic residues at binding site I derived from the structural model.

Taken together, an iterative approach combining site-directed mutagenesis and comparative modeling of the binding pocket of nicotinic acid at GPR109A identified five residues as main interaction points. The binding pocket is located between the basic anchor site at TMH3 (Arg111) for the acidic group of the ligand and the interaction site for the ring system of the ligands formed by the junction TMH2/ECL1 (Asn86, Trp91), TMH7 (Phe276, Tyr284), and the tip of ECL2 (Ser178).

Discussion

Based on the remarkable clinical effects of nicotinic acid, its recently discovered G-protein-coupled receptor represents one of the prime targets for the development of new antidyslipidemic drugs (Pike and Wise, 2004). Major aims of new drug development in this field are, for example, the improvement of the relatively low potency and unfavourable pharmacokinetic properties of nicotinic acid. In addition, a better ratio of wanted and unwanted effects would be desirable. To understand more about the structural requirements for binding of ligands to the nicotinic acid receptor, we have characterized the binding site on the human nicotinic acid receptor GPR109A. We were surprised to find that our data indicate that the binding site of GPR109A for its known pharmacological small molecule ligands differs from the traditional binding site of class A G-protein-coupled receptors for small molecule ligands, which in the case of biogenic amine receptors is located between TMH3, TMH5, and TMH6 (Strader et al., 1994; Gether, 2000; Kristiansen, 2004). Our major new finding is that the binding crevice of GPR109A for nicotinic acid seems to be formed by the TMH2, TMH3, and TMH7, and both the junction TMH2/ECL1 and ECL2 critically contribute to ligand binding. Chimera studies combined with re-introduction of single amino acid changes indicated that Asn86/Trp91 at the junction TMH2/ECL1 and Ser178 at ECL2 are essential determinants for nicotinic acid binding to GPR109A.

The common feature of all known ligands of GPR109A is the presence of a carboxylic group, suggesting that this acidic group is critically involved in binding. This is supported by the fact that any change or substitution at the carboxylic acid moiety of nicotinic acid, such as in nicotinamide, completely abrogates its pharmacological activity. Based on the assumption that the carboxylic acid group forms a salt bridge with a residue in one of the TM regions of the receptors, we searched for positively charged residues that would allow for an electrostatic interaction with the carboxyl oxygens. Of four candidate arginine residues in TMHs 3, 6, and 7, only arginine 111 in TMH3 was absolutely required for binding of nicotinic acid to GPR109A. In contrast, mutational deletion of positively charged residues in TMH6 and -7 did not interfere with the ability of the receptor to bind nicotinic acid. It is noteworthy that the recently discovered dicarboxylic acid receptor GPR91 has been suggested to require positively charged amino acid residues in TMH 6 and 7; two residues in TMH3 (He et al., 2004) and an arginine residue in TMH7 of prostanoid receptors have been suggested to bind to the C1-carboxylate of prostanoids (Stitham et al., 2003).

Class A GPCRs for small molecule agonists bind their specific ligands via the extracellular half of their 7 TM domain. Multiple mutagenesis experiments and molecular modeling structures clearly indicate that the binding sites for most small molecule agonists, such as biogenic amines, are located between TMH3, -4, -5, -6, and -7 (Strader et al., 1994; Ji et al., 1998; Bonini et al., 2000; Shi and Javitch, 2002; Stenkamp et al., 2002; Kristiansen, 2004). Our findings support a structural model for GPR109A in which the nicotinic acid binding pocket is localized between TMH2, -3, and -7. The ligands of various receptors, such as the C3a receptor (Kim et al., 1999), the Ca^{2+}-sensing receptor (Miedlich et al., 2004), the prostacyclin receptor (Stitham et al., 2003), or the vasopressin V_2 receptor (Wuller et al., 2004), are also interacting with a similar binding site on their respective receptors.

TABLE 2

Nicotinic acid and acifran evoked Ca^{2+} responses (EC_{50}) and nicotinic acid binding affinity (K_d) for aromatic residue mutants of GPR109A

Shown are data for the indicated GPR109A mutants. The EC_{50} values of nicotinic acid-induced increases in $[Ca^{2+}]_i$ were determined in CHO-K1 cells expressing $G\alpha_{15}$ and the indicated wild-type or mutant receptors. The K_D and B_{max} values were determined by Scatchard analysis of [^{3}H]nicotinic acid binding saturation isotherms and represent the mean ± S.D. of at least three independent experiments. Relative cell surface expression levels of wild-type and GPR109A receptor mutants were determined by ELISA assay in nonpermeabilized CHO-K1 cells (see *Materials and Methods*).

GPR109A Mutants	EC_{50}		[^{3}H] Nicotinic Acid Binding		Surface Expression
	Nicotinic Acid	Acifran	K_d	B_{max}	
	μM		*nM*	*pmol/mg*	*RLU*
F180A	>100	>100	>500		40.78 ± 2.5
F180L	1.8 ± 0.2	5.4 ± 6			
F193A	>100	>100	>500		42.2 ± 3.9
F193L	4 ± 0.6	8 ± 2			
F276A	>100	>100	>500		39.96 ± 4.1
F276L	>100	>100	>500		37.88 ± 2.4
Y284A	81 ± 17	>100	300 ± 36	3.60 ± 0.42	39.91 ± 3.7
Y284L	153 ± 10	>100	342 ± 40	3.75 ± 0.39	39.08 ± 4.5

Although the major binding sites for small molecule ligands of GPCRs are localized in the TM helices, there is evidence from site-directed mutagenesis experiments that certain residues in ECL2 can also particularly contribute to binding of small ligands to GPCRs (Kim et al., 1996; Zhao et al., 1996; Shi and Javitch, 2004). Similar to many other GPCRs, GPR109A as well has a disulfide bond between ECL2 (C177) and TMH3 (C100). Because of the disulfide linkage, ECL2 is constrained over the ligand binding pocket, and residues from ECL2 can take part in ligand binding. In our model, Ser178 of ECL2 reaches into the ligand binding pocket and interacts with the nitrogen of the pyridine ring of nicotinic acid.

As already reported for other GPCRs (Balmforth et al., 1997; Groblewski et al., 1997), in our homology model of GPR109A, the inactive state is also restrained by side-chain interactions between TMH3 and TMH6/TMH7, where Arg111 (TMH3) is very likely to be involved in side-chain interactions with Ser247 (TMH6) and Thr283 (TMH7), stabilizing/constraining the inactive conformation. Arginine 111 at TMH3 is the pivotal residue for electrostatic recognition and binding, and it functions as a basic anchor point for the acidic group of the ligands. Our findings support a scenario in which the arginine side chain is forced to delocalize from its inactive state orientation. The positively charged guanidine group of the arginine side chain moves toward the negatively charged acid group of the ligand upon binding, and the interaction between helices TMH3 and TMH6/TMH7 is weakened or lost.

According to several X-ray structures of nicotinic acid/protein complexes, in which nicotinic acid is surrounded by aromatic residues (Reddy et al., 1996; Ellis et al., 1997; Cheong et al., 1999, 2001; Lovering et al., 2001), and based on our docking model of nicotinic acid/GPR109A, the participation of aromatic residues as direct and indirect partners in the binding site was predicted. To distinguish between direct and indirect aromatic interaction partners of the ligand, we introduced strong (alanine) and weak (leucine) alterations of side-chain properties by mutations. Mutants of Phe276 and Tyr284 showed identical strong effects for alanine and leucine as well, indicating a direct aromatic interaction of both positions on ligand binding. Whereas the common differences between alanine and leucine mutants for Phe180 and Phe193 indicate rather indirect effects of the two residues on ligand binding. Leucine mutants are preserving the necessary hydrophobic properties needed for proper orientation of the neighbored side chains. The strong side chain reduction in size and hydrophobicity in case of alanine mutants may lead to slightly altered assembly of the neighboring side chains and/or helices and thus may indirectly affect the proper shape and size of the ligand binding site. Finally, all residues experimentally identified as essential direct interaction partners are located in the GPR109A model in very close spatial proximity and provide support that the binding site of nicotinic acid is located between TMH3, junction TMH2/ECL1, TMH7, and the tip of ECL2. The data combined with the model suggest also the possibility that some aromatic residues, such as Trp91 and Phe276, play a role in the formation of a gateway that allows nicotinic acid to access the binding pocket.

Taking advantage of the high degree of sequence homology between the human high-affinity nicotinic acid receptor GPR109A and the receptor GPR109B, which has only very low affinity for nicotinic acid, we have identified critical residues for the binding of nicotinic acid to GPR109A. By combining mutagenesis data and comparative structural modeling, we were able to identify five residues located in close spatial proximity as the main interaction points for nicotinic acid. The characterization of the structural determinants and complementary pharmacophoric patterns for binding of nicotinic acid at GPR109A is of general importance for understanding the binding mechanism of small molecule ligands to GPCRs as well as for the design and development of new drugs acting via GPR109A to treat dyslipidemic disorders.

Acknowledgments

We thank R. LeFaucheur for help with the manuscript.

References

Aktories K, Schultz G, and Jakobs KH (1980) Regulation of adenylate cyclase activity in hamster adipocytes. Inhibition by prostaglandins, alpha-adrenergic agonists and nicotinic acid. *Naunyn-Schmiedeberg's Arch Pharmacol* **312:**167–173.

Aktories K, Schultz G, and Jakobs KH (1982) Inactivation of the guanine nucleotide regulatory site mediating inhibition of the adenylate cyclase in hamster adipocytes. *Naunyn-Schmiedeberg's Arch Pharmacol* **321:**247–252.

Altschul R, Hoffer A, and Stephen JD (1955) Influence of nicotinic acid on serum cholesterol in man. *Arch Biochem* **54:**558–559.

Ballesteros JA and Weinstein H (1992) Analysis and refinement of criteria for predicting the structure and relative orientations of transmembranal helical domains. *Biophys J* **62:**107–109.

Balmforth AJ, Lee AJ, Warburton P, Donnelly D, and Ball SG (1997) The conformational change responsible for AT1 receptor activation is dependent upon two juxtaposed asparagine residues on transmembrane helices III and VII. *J Biol Chem* **272:**4245–4251.

Baubet V, Le Mouellic H, Campbell AK, Lucas-Meunier E, Fossier P, and Brulet P (2000) Chimeric green fluorescent protein-aequorin as bioluminescent Ca^{2+} reporters at the single-cell level. *Proc Natl Acad Sci USA* **97:**7260–7265.

Berman HM, Westbrook J, Feng Z, Gilliland G, Bhat TN, Weissig H, Shindyalov IN, and Bourne PE (2000) The Protein Data Bank. *Nucleic Acids Res* **28:**235–242.

Blum CB, Levy RI, Eisenberg S, Hall M 3rd, Goebel RH and Berman M (1977) High density lipoprotein metabolism in man. *J Clin Investig* **60:**795–807.

Bonini JA, Jones KA, Adham N, Forray C, Artymyshyn R, Durkin MM, Smith KE, Tamm JA, Boteju LW, Lakhlani PP, et al. (2000) Identification and characterization of two G protein-coupled receptors for neuropeptide FF. *J Biol Chem* **275:**39324–39331.

Carlson LA and Oro L (1962) The effect of nicotinic acid on the plasma free fatty acid; demonstration of a metabolic type of sympathicolysis. *Acta Med Scand* **172:**641–645.

Case DA, Pearlman DA, Caldwell JW, Cheatham TE, Wang J, Ross WS, Simmerling CL, Darden TA, Merz KM, Stanton RV, et al. (2002) AMBER 7 program, University of California, San Francisco.

Cayen MN, Kallai-Sanfacon MA, Dubuc J, Greselin E, and Dvornik D (1982) Effect of AY-25,712 on fatty acid metabolism in rats. *Atherosclerosis* **45:**281–290.

Cheong CG, Escalante-Semerena JC, and Rayment I (1999) The three-dimensional structures of nicotinate mononucleotide:5,6- dimethylbenzimidazole phosphoribosyltransferase (CobT) from Salmonella typhimurium complexed with 5,6-dimethybenzimidazole and its reaction products determined to 1.9 A resolution. *Biochemistry* **38:**16125–16135.

Cheong CG, Escalante-Semerena JC, and Rayment I (2001) Structural investigation of the biosynthesis of alternative lower ligands for cobamides by nicotinate mononucleotide: 5,6-dimethylbenzimidazole phosphoribosyltransferase from Salmonella enterica. *J Biol Chem* **276:**37612–37620.

Ellis PJ, Appleby CA, Guss JM, Hunter WN, Ollis DL, and Freeman HC (1997) Structure of ferric soybean leghemoglobin a nicotinate at 2.3 A resolution. *Acta Crystallogr D Biol Crystallogr* **53:**302–310.

Gether U (2000) Uncovering molecular mechanisms involved in activation of G protein-coupled receptors. *Endocr Rev* **21:**90–113.

Groblewski T, Maigret B, Larguier R, Lombard C, Bonnafous JC, and Marie J (1997) Mutation of Asn111 in the third transmembrane domain of the AT1A angiotensin II receptor induces its constitutive activation. *J Biol Chem* **272:**1822–1826.

He W, Miao FJ, Lin DC, Schwandner RT, Wang Z, Gao J, Chen JL, Tian H, and Ling L (2004) Citric acid cycle intermediates as ligands for orphan G-protein-coupled receptors. *Nature (Lond)* **429:**188–193.

Ji TH, Grossmann M, and Ji I (1998) G protein-coupled receptors. I. Diversity of receptor-ligand interactions. *J Biol Chem* **273:**17299–17302.

Kim IS, Kim ER, Nam HJ, Chin MO, Moon YH, Oh MR, Yeo UC, Song SM, Kim JS, Uhm MR, et al. (1999) Activating mutation of GS alpha in McCune-Albright syndrome causes skin pigmentation by tyrosinase gene activation on affected melanocytes. *Horm Res* **52:**235–240.

Kim J, Jiang Q, Glashofer M, Yehle S, Wess J, and Jacobson KA (1996) Glutamate residues in the second extracellular loop of the human A2a adenosine receptor are required for ligand recognition. *Mol Pharmacol* **49:**683–691.

Knopp RH (1999) Drug treatment of lipid disorders. *N Engl J Med* **341:**498–511.

Kristiansen K (2004) Molecular mechanisms of ligand binding, signaling and regulation within the superfamily of G-protein-coupled receptors: molecular modeling and mutagenesis approaches to receptor structure and function. *Pharmacol Ther* **103:**21–80.
LaRosa JC, Miller VT, Edwards KD, DeBovis MR, and Stoy DB (1987) Acifran: a double-blind, randomized, placebo-controlled efficacy study in type IIa hyperlipoproteinemic patients. *Artery* **14:**338–350.
Laskowski RA, Rullmannn JA, MacArthur MW, Kaptein R, and Thornton JM (1996) AQUA and PROCHECK-NMR: programs for checking the quality of protein structures solved by NMR. *J Biomol NMR* **8:**477–486.
Lovering AL, Hyde EI, Searle PF, and White SA (2001) The structure of Escherichia coli nitroreductase complexed with nicotinic acid: three crystal forms at 1.7 A, 1.8 A and 2.4 A resolution. *J Mol Biol* **309:**203–213.
Miedlich SU, Gama L, Seuwen K, Wolf RM, and Breitwieser GE (2004) Homology modeling of the transmembrane domain of the human calcium sensing receptor and localization of an allosteric binding site. *J Biol Chem* **279:**7254–7263.
Noda K, Saad Y, Graham RM, and Karnik SS (1994) The high affinity state of the β2-adrenergic receptor requires unique interaction between conserved and non-conserved extracellular loop cysteines. *J Biol Chem* **269:**6743–6752.
Olsson AG (1994) Nicotinic acid and derivatives, in *Principles and Treatment of Lipoprotein Disorders* (Schettler G and Habenicht AJR eds) pp 349–400, Handbook of Experimental Pharmacology, vol. 109, Springer-Verlag, Heidelberg.
Pike NB and Wise A (2004) Identification of a nicotinic acid receptor: is this the molecular target for the oldest lipid-lowering drug? *Curr Opin Investig Drugs* **5:**271–275.
Reddy SG, Scapin G, and Blanchard JS (1996) Interaction of pyridine nucleotide substrates with Escherichia coli dihydrodipicolinate reductase: thermodynamic and structural analysis of binary complexes. *Biochemistry* **35:**13294–13302.
Sansom MS and Weinstein H (2000) Hinges, swivels and switches: the role of prolines in signalling via transmembrane alpha-helices. *Trends Pharmacol Sci* **21:**445–451.
Savarese TM, Wang CD, and Fraser CM (1992) Site-directed mutagenesis of the rat m1 muscarinic acetylcholine receptor. Role of conserved cysteines in receptor function. *J Biol Chem* **267:**11439–11448.
Shepherd J, Packard CJ, Patsch JR, Gotto AM Jr, and Taunton OD (1979) Effects of nicotinic acid therapy on plasma high density lipoprotein subfraction distribution and composition and on apolipoprotein A metabolism. *J Clin Investig* **63:**858–867.
Shi L and Javitch JA (2002) The binding site of aminergic G protein-coupled receptors: the transmembrane segments and second extracellular loop. *Annu Rev Pharmacol Toxicol* **42:**437–467.
Shi L and Javitch JA (2004) The second extracellular loop of the dopamine D2 receptor lines the binding-site crevice. *Proc Natl Acad Sci USA* **101:**440–445.
Soga T, Kamohara M, Takasaki J, Matsumoto S, Saito T, Ohishi T, Hiyama H, Matsuo A, Matsushime H, and Furuichi K (2003) Molecular identification of nicotinic acid receptor. *Biochem Biophys Res Commun* **303:**364–369.
Stenkamp RE, Filipek S, Driessen CA, Teller DC, and Palczewski K (2002) Crystal structure of rhodopsin: a template for cone visual pigments and other G protein-coupled receptors. *Biochim Biophys Acta* **1565:**168–182.
Stitham J, Stojanovic A, Merenick BL, O'Hara KA, and Hwa J (2003) The unique ligand-binding pocket for the human prostacyclin receptor. Site-directed mutagenesis and molecular modeling. *J Biol Chem* **278:**4250–4257.
Strader CD, Fong TM, Tota MR, Underwood D, and Dixon RA (1994) Structure and function of G protein-coupled receptors. *Annu Rev Biochem* **63:**101–132.
Teller DC, Okada T, Behnke CA, Palczewski K, and Stenkamp RE (2001) Advances in determination of a high-resolution three-dimensional structure of rhodopsin, a model of G-protein-coupled receptors (GPCRs). *Biochemistry* **40:**7761–7772.
ter Laak AM and Kuhne R (1999) Bacteriorhodopsin in a periodic boundary water-vacuum-water box as an example towards stable molecular dynamics simulations of G-protein coupled receptors. *Recept Channels* **6:**295–308.
Tornvall P, Hamsten A, Johansson J, and Carlson LA (1990) Normalisation of the composition of very low density lipoprotein in hypertriglyceridemia by nicotinic acid. *Atherosclerosis* **84:**219–227.
Tunaru S, Kero J, Schaub A, Wufka C, Blaukat A, Pfeffer K, and Offermanns S (2003) PUMA-G and HM74 are receptors for nicotinic acid and mediate its anti-lipolytic effect. *Nat Med* **9:**352–355.
Wise A, Foord SM, Fraser NJ, Barnes AA, Elshourbagy N, Eilert M, Ignar DM, Murdock PR, Steplewski K, Green A, et al. (2003) Molecular identification of high and low affinity receptors for nicotinic acid. *J Biol Chem* **278:**9869–9874.
Wuller S, Wiesner B, Loffler A, Furkert J, Krause G, Hermosilla R, Schaefer M, Schulein R, Rosenthal W, and Oksche A (2004) Pharmacochaperones post-translationally enhance cell surface expression by increasing conformational stability of wild-type and mutant vasopressin V2 receptors. *J Biol Chem* **279:**47254–47263.
Zellner C, Pullinger CR, Aouizerat BE, Frost PH, Kwok PY, Malloy MJ, and Kane JP (2005) Variations in human HM74 (GPR109B) and HM74A (GPR109A) niacin receptors. *Hum Mutat* **25:**18–21.
Zhao MM, Hwa J, and Perez DM (1996) Identification of critical extracellular loop residues involved in α1-adrenergic receptor subtype-selective antagonist binding. *Mol Pharmacol* **50:**1118–1126.

Address correspondence to: Stefan Offermanns, Institute of Pharmacology, University of Heidelberg, Im Neuenheimer Feld 366, 69120 Heidelberg, Germany. E-mail: stefan.offermanns@urz.uni-heidelberg.de